General and Comparative Endocrinology 330 (2023) 114128

Contents lists available at ScienceDirect

General and Comparative Endocrinology

journal homepage: www.elsevier.com/locate/ygcen

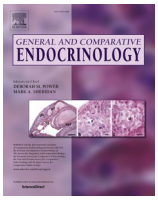

Eyestalk neuropeptide identification in the female red deep-sea crab, *Chaceon quinquedens*

Shadaesha Green, Tsvetan Bachvaroff, J. Sook Chung *

Institute of Marine and Environmental Technology, University of Maryland Center for Environmental Science, 701 E. Pratt Street, Baltimore, MD 21202, USA

ARTICLE INFO

Keywords:
Crustacean hyperglycemic hormone
Molt-inhibiting hormone
Eyestalk neuropeptides
Vitellogenesis
Transcriptome analysis
Red deep-sea crabs

ABSTRACT

Eyestalk-derived neuropeptides, primarily the crustacean hyperglycemic hormone (CHH) neuropeptide family, regulate vitellogenesis in decapod crustaceans. The red deep-sea crab, *Chaceon quinquedens,* a cold-water species inhabiting depths between 200 and 1800 m, has supported a small fishery, mainly harvesting adult males in the eastern US for over 40 years. This study aimed to understand the role of eyestalk-neuropeptides in vitellogenesis in *C. quinquedens* with an extended intermolt stage. Chromatography shows two CHH and one MIH peak in the sinus gland, with a CHH2 peak area four times larger than CHH1. The cDNA sequence of MIH and CHH of *C. quinquedens* is isolated from the eyestalk ganglia, and the qPCR assay shows *MIH* is significantly higher only at ovarian stages 3 than 4 and 5. However, *MIH* transcript and its neuropeptides do differ between stages 1 and 3. While *CHH* transcripts remain constant, its neuropeptide levels are higher at stages 3 than 1. Additionally, transcriptomic analysis of the *de novo* eyestalk ganglia assembly at ovarian stages 1 and 3 found 28 eyestalk neuropeptides. A GIH/VIH or GSH/VSH belonging to the CHH family is absent in the transcriptome. Transcripts per million (TPM) values of ten neuropeptides increase by 1.3 to 2.0-fold at stage 3 compared to stage 1: twofold for Bursicon α, followed by CHH, AKH/corazonin-like, Pyrokinin, CCAP, Glycoprotein B, PDH1, and IDLSRF-like peptide, and 1.3-fold of allatostatin A and short NP-F. WXXXRamide, the only downregulated neuropeptide, decreases TPM by ~ 2-fold at stage 3, compared to stage 1. Interestingly, neuroparsin with the highest TPM values remains the same in stages 1 and 3. The mandibular organ-inhibiting hormone is not found in *de novo* assembly. We report that CHH, MIH, and eight other neuropeptides may play a role in vitellogenesis in this species.

1. Introduction

The Atlantic red deep-sea crab, *Chaceon quinquedens* inhabits the Atlantic Ocean coastal waters from Nova Scotia to the Gulf of Mexico at depths and temperatures ranging from 200 − 1800 m and from 5 to 8 °C, respectively (Chute et al., 2008; Haefner and Musick, 1974; Steimle et al., 2001; Weinberg and Keith, 2003). It has supported a small commercial fishery along the eastern US (from the Gulf of Maine to Cape Hatteras, NC) since the early 1970 s (Wahle et al., 2008; Wigley et al., 1975). Currently the *C. quinquedens* fishing industry harvests adult males based on size, with carapace widths>94 mm (Chute et al., 2008), while females are protected from harvesting. The reproductive biology of *C. quinquedens* with a life span of up to 15 years (Serchuk and Wigley, 1982), is largely unknown. Studies report that females exhibit a biennial reproductive cycle (Erdman et al., 1991; Hilário and Cunha, 2013; Martínez-Rivera and Stevens, 2020; Stevens and Guida, 2016), indicating a long-period vitellogenesis, and possibly a year-long embryogenesis like *Chionoecetes opilio* (Webb et al., 2007).

Vitellogenesis takes place in the hepatopancreas and ovary of decapod crustaceans and is known to be regulated largely by the neuropeptide hormone(s) derived from the eyestalk ganglia (Chen et al., 2018, 2014; Tsutsui et al., 2013; Zmora et al., 2009b, 2009a). Such neuropeptides referred to as vitellogenesis-inhibiting/stimulating hormones (VI/SH) in shrimp and lobsters belong to the crustacean hyperglycemic hormone (CHH) superfamily (Chan et al. 2003). In crab species, the multifunctional hormone CHH has a role in vitellogenesis, whereas lobsters and shrimp utilize a specific structural form of VI/SH (Chen et al., 2014; Chen et al., 2020; Kluebsoongnoen et al., 2020; Vijayan et al., 2013).

In decapod crustaceans, the X-organ and sinus gland located in the eyestalk ganglia synthesizes and releases these neuropeptides, respectively. But the neuropeptide profiles differ by species, including

* Corresponding author.
E-mail address: chung@umces.edu (J. Sook Chung).

https://doi.org/10.1016/j.ygcen.2022.114128
Received 21 November 2021; Received in revised form 9 September 2022; Accepted 16 September 2022
Available online 21 September 2022

structural variation in VI/SH or CHH. The SG of *C. quinquedens* is expected to have a neuropeptide profile similar to the green crab, *Carcinus maenas*, and *Callinectes sapidus* (Chung and Webster, 1996; Zmora and Chung, 2014), with two structural isoforms of CHH and a single MIH.

Additionally, the molt-inhibiting hormone (MIH), another CHH superfamily member, also exhibits vitellogenesis-stimulating action in some species (Zmora et al., 2009b, 2009a; Tiu and Chan, 2007). MIHs main role is to suppress the Y-organ (YO) inhibiting synthesis and secretion of molting hormones in crustaceans (Chen et al., 2020; Mykles and Chang, 2020). In the blue crab, *C. sapidus*, only females experience a puberty-terminal molt and remain at the intermolt stage for the remaining reproductively active stage of their lives, while males continue molting after reaching adulthood. In such case, MIH plays a dual role: halting the animal at intermolt by maintaining low hemolymph ecdysone levels and simultaneously stimulating vitellogenesis in the hepatopancreas (Zmora et al., 2009b, 2009a). Given this, it is plausible to suggest that the MIH in the female adult *C. quinquedens* that experience a 2–7 yearlong molt cycle (Gerrior, 1981; Lux et al., 1982) may play a similar dual role in regulating molting and stimulating vitellogenesis (Zmora et al., 2009b, Zmora et al., 2009a).

RNA sequencing (RNA-seq) has become a widely used tool for obtaining an overview of many physiological processes and gene discovery. Transcriptomic analysis has been used to identify putative neuropeptides in eyestalks of *Eriocheir sinensis* (Xu et al. 2015; Pang et al. 2019), *Homarus americanus* (Christie et al., 2017), *Litopenaeus vannamei* (Wei et al., 2020), *Macrobrachium rosenbergii* (Suwansa-Ard et al., 2015), *Portunus trituberculatus* (Lv et al., 2017), and *Procambarus clarkii* (Manfrin et al., 2015). The neuropeptides that may have reproductive functions are also reported in *Scylla paramamosain* (Bao et al., 2015; Gao et al., 2014), *E. sinensis* (Liu et al., 2019), *M. nipponense* (Qiao et al., 2017; Zhang et al., 2021), *P. trituberculatus* (Meng et al., 2015), *L. vannamei* (Wang et al., 2019), *Nephrops norvegicus* (Rotllant et al., 2018), *Sagmariasus verreauxi* (Ventura et al., 2014), and *Cherax quadricarinatus* (Nguyen et al., 2016).

This study aimed to understand the role of eyestalk neuropeptide(s) in vitellogenesis. To this end, MIH and CHH cDNA sequences were first isolated from the eyestalk ganglia of *C. quinquedens* using traditional cloning methods and their expression was quantified in the eyestalk ganglia at various ovarian stages. *De novo* transcriptome assembly of the eyestalk ganglia was conducted to determine if transcripts of other neuropeptides differ by ovarian stages.

2. Materials and methods

2.1. Animals

Adult female and male *C. quinquedens* at intermolt stage were collected from the mid-Atlantic Bight region of the United States off the coast of Virginia up to Massachusetts. Samples were collected in the summer of 2013 onboard the NOAA R/V the Gordon Gunter and onboard the F/V Hannah Boden (29 m) in 2014 and 2015. We chose carapace length (CL) as the unit of measurement for the body size and these animals (Stevens and Guida, 2016) were 78 ± 2 mm (n = 5/group) for the expression analysis. An eyestalk from each female was removed, and two small cuts were placed on each side of the eyestalk. The eyestalk was placed in a 1.5 mL microcentrifuge tube containing 500 μl of RNA*later*® Solution (Ambion®). Samples were then stored at −80℃ until further processing. The remaining eyestalk was placed in a 1.5 mL microcentrifuge tube containing 1 mL Stefanini fixative (Stefanini et al., 1967).

Ovarian stages were determined according to the criteria described in (Haefner, 1977; Huang et al., 2020; Martínez-Rivera et al., 2020). In brief, ovary color and size were key parameters used to stage the ovary. Ovary stage by color is as follows, early (stage 1; colorless or white to beige), intermediate (stage 2; yellow to light orange), advanced (stage 3; bright orange to brown), mature (stage 4; red orange to purple), and redeveloping (stage 5; beige).

2.2. Separation of SG neuropeptides and dot blot assay

For the levels of CHH and MIH neuropeptides in the SG of adult males and females *C. quinquedens* (~90 mm CL) were obtained from the Atlantic Red Crab Company (New Bedford, MA), including adult females (ovarian stage 2 and 3; n = 9) and males (n = 11). A single SG of each animal was dissected and stored at −80 °C until processed. The supernatant of a single SG that was briefly sonicated for 10 *sec* (Branson Sonifier 450) in 100 μl ice-cold 2 N acetic acid and then centrifuged at 14,000 rpm for 3 min, then was separated on a Jupiter C18 column (4.6 × 150 mm, 5 μm, Phenomenex) connected to an RP-HPLC (Agilent 1100) at the gradient conditions stated in (Chung and Webster, 1996; Zmora and Chung, 2014). Relative amounts of neuropeptides in a SG were calculated using chromatogram peak areas at 210 nm absorption, as reported for *C. borealis* (Chung et al., 2020). The major peaks were also collected manually and dried in a SpeedVac (Jouan) for a dot-blot assay. The peaks were tested using anti-*Callinectes* MIH and anti-*Carcinus* CHH sera to detect MIH and CHH cross-reactivity, respectively (Chung, 2004; Zmora et al., 2009a).

2.3. Localization of CHH family neuropeptides in the eyestalk

Whole-mount immunohistochemistry was used to localize CHH in the SG and X-organ neurosecretory cells of eyestalk ganglia (Chung and Webster, 2004). First, eyestalk ganglia stored in Stefanini fixative were carefully dissected under a dissecting microscope (Stefanini et al., 1967). Eyestalks were then washed in phosphate buffer containing Triton X (PTX) (50 mM phosphate buffer + 0.5 % Triton X + 0.01 % sodium azide) 5 times for 30 min each and then incubated with *anti-Carcinus* CHH (Chung and Webster, 2004) serum at a final dilution of 1:1000 for 3 days at 4 °C. Next, a goat-anti rabbit-IgG labeled with Alexa 488 (x150 fold diluted in PTX) was applied to the samples after repeating the washing step. Finally, the images were collected using a Z-stack with a confocal microscope (BioRad Radiance 2100 system).

2.4. Isolation of CHH neuropeptide cDNA sequence

Total RNA from three eyestalks of adult females at ovarian stage 3 was extracted using QIAzol reagent (Qiagen) following the manufacturer's protocol. RNA quality and quantity were determined using a NanoDrop (Thermo Scientific, MA). One to 1.5 μg of total RNA was used to synthesize 5′ and 3′ RACE cDNAs using a SMART™ cDNA synthesis kit (TaKaRa,). A two-step PCR was employed by following the procedures as described (Chung et al., 2009; Vinagre et al., 2020; Vinagre and Chung, 2016; Zmora et al., 2009a) using the list of degenerate and gene-specific (Table 1) primers for *MIH*, *CHH*, and *vitellogenin* (*VTG*), with arginine kinase. Gene-specific primers were generated based on the initial sequencing and used for 5′ and 3′ RACE by following the procedures as described (Chung et al., 2012, Chung et al., 2009).

2.5. Sequence analysis and phylogenetic tree analysis

The full-length *CHH* and *MIH* nucleotide sequences were examined using NCBI BLASTX. Open reading frames (ORF) were identified via ORF finder (https://www.ncbi.nlm.nih.gov/orffinder/). The SignalP v.5.0 Server was used to determine the presence of a signal peptide (http://www.cbs.dtu.dk/services/SignalP/). RNA regulatory motifs were determined by examining the 5′ and 3′ UTR regions using RegRNA (http://regrna.mbc.nctu.edu.tw/index1.php, Huang et al., 2006). Microsatellite Repeats Finder (http://insilico.ehu.es/mini_tools/microsatellites/?info) was used to identify microsatellite regions in the 3′UTR of *MIH*. The ORF sequences were also confirmed using a high fidelity Taq polymerase (Clonetch).

BLAST hits with>75 % sequence identity to other crab or decapod MIHs and CHHs (Supplemental Data 1A and B) were selected and

Table 1
List of primers for isolating the cDNA sequence of *CHH, MIH*, *VTG,* and *AK* from the eyestalk of female *C. quinquedens* and qPCR assays.

Primer Name	Primer sequences (5′ to 3′)
CHHdF1	TGYAARGGNGTNTAYGA
CHHdF2	CATRCAYTGNCKRAANAC
CHHdR1	GAYTTYATHGCNGCNGGNAT
MIHdF1	GNGTNATHAAYGAYGA
MIHdF2	TGYCCNAAYYTNATHGGNAA
MIHdR1	AARTCYTCRTTRAARAARCA
AKdF1	CAYTTYYTNTTYAARGARGG
AKdF2	AAYGCNTGYMGNTAYTGGCC
AKdR1	CCNCCYTCNGCYTCNGTRTG
ChqAK-QF	CTGGGCCAGGTATACCGCCGCCTTGTCAGC
ChqAK-QR	GGGGAGCTTGATGTGGACGGAGGCACGCAC
ChqMIH-QF2	GAACAGAGACCTTTATAAGAAAGTAGAGTG
ChqMIH-QR2	CTGACCCACCGCTTCAACTGTGTCATCTCT
ChqChh-QF1	CGATCAGCGCAAGGATTAAGAATGGAGCGG
ChqChh-QR2	CCAGGTCGCTGAACAGGCCACGGTCATACA
TaqvitF	TGTACAGCTGAAAGGCGTGG
TaqvitR	CATGGGCCGAGAACAGTCA
ChqVTG-QF	ATCTCCCGCATTGGTCAGGACCAGCTGGTG
ChqVTG-QR	GGCATCGGCTTCAACTCCATCCCTGGTGAT

d = degenerate primers; Q = primers used for qPCR assays.

aligned using MAFFT, trimmed with GBLOCKS, and analyzed using PhyML with 100 bootstrap replicates as implemented by the phylogeny.fr website (https://www.phylogeny.fr).

2.6. Transcript levels of CHH, MIH, and VTG using qPCR assays

One to 1.5 μg of each eyestalk or hepatopancreas total RNA sample from adults with (78 ± 2 mm, CL) females (ovarian stages 2–5; n = 5/stage) and male eyestalk ganglia (101 ± 1 mm, CL, n = 5) was reverse transcribed using a PrimeScript™ reagent kit with gDNA Eraser (TaKaRa) following the manufacturer's protocol. Each standard (*MIH, CHH, VTG,* and *AK*) was generated as described (Chung et al., 2012, 2009). Transcript levels were estimated using cDNA samples (25 ng total RNA equivalent) in duplicate with Fast SYBR Green Master Mix (Life Technologies) on an Applied Biosystems 7500 Real-Time PCR System (Chung et al., 2012, Chung et al., 2009).

2.7. Sample preparation and Illumina sequencing

Total RNA was extracted and quantified from the eyestalks of females at ovarian stages 1 and 3, as described above. Total RNA from three females at each stage (carapace length ≥ 73 mm) was pooled with an equal concentration. Pooled total RNA was used for library preparation and paired end 150 base sequencing on the Illumina HiSeq 2500 platform (Macrogen).

2.8. De novo assembly and neuropeptide mining

The *de novo* assembly software Trinity (v. 2.8.6) was used to assemble paired-read sequences using the default parameters (including -trimmomatic to clean reads and no read normalization) (Grabherr et al., 2011; Haas et al., 2013). The completeness of the assembly was evaluated using the Benchmarking Universal Single-Copy Orthologs (BUSCO) approach by aligning to the arthropod reference set (Simão et al., 2015). Expression levels of the transcripts in the assembly were estimated by remapping the high-quality reads on both transcriptomes separately with RNA-Seq by Expectation-Maximization (Robinson et al., 2010, Li and Dewey, 2011). RSEM data for both stages were further analyzed to determine the most highly expressed sequences. Additionally, differential expression using edgeR at p-value (0.05) and log fold change > 2 was used.

The eyestalk transcriptome was mined for several neuropeptides using a well-established workflow (Christie, 2016, 2015, 2014a; Christie et al., 2017, 2008; Christie and Pascual, 2016; Ma et al., 2010). The amino acid sequences of 53 eyestalk-neuropeptides from different decapod species were collected and placed in a text file using NCBIs efetch utility a command line (Supplemental data 2). These sequences were then BLASTed against the eyestalk assembly using an e-value cut-off 1e-30. Transcript per million (TPM) values for the neuropeptides reported were extracted from the RSEM data to examine differences between ovarian stages.

Candidate neuropeptide nucleotide sequences were then compared to GenBank using BLASTX (https://blast.ncbi.nlm.nih.gov/). As described above, contigs detected as neuropeptides were translated using ExPASy Translate (web.expasy.org/translate) and signal peptides were identified with SignalP v.5.0 Server (http://www.cbs.dtu.dk/services/SignalP/).

2.9. Statistical analysis

The statistical significance of each dataset was examined using a one-way ANOVA with the post-hoc Kruskal-Wallis test or a Student's *t* test. Significant differences were accepted at $P < 0.05$ and noted with different letters and asterisk. The data are presented as mean ± SE (n), where 'n' is the number of animals.

3. Results

3.1. Identification of CHH, MIH and their levels in the SG and the localization of CHH in the eyestalk ganglia

The three peaks that were manually collected from an RP-HPLC and labeled as 1, 2, and 3 were cross-reacted with anti-*Carcinus* CHH and -*Callinectes* MIH sera and referred to as CHH1 (no. 1), CHH2 (no. 2) and MIH (no.3) (Fig. 1A; noted with a dot under the peak).

A potential function of CHH and MIH in vitellogenesis was examined by comparing their levels in the SG of adult females (n = 10) and males (n = 11). As shown in Fig. 1B, the neuropeptide peak area (m*AU) was ranked: the highest was CHH2 with 5143 ± 523 in females, significantly higher ($P < 0.05$) than 3594 ± 489 in males. The CHH precursor-related peptide (CPRP) had a peak area of 2222 ± 22 in females and 1768 ± 223 in males, while CHH1 was 918 ± 74 in females and 893 ± 133 in males. MIH was 895 ± 57 in females and 795 ± 102 in males. The ratio of CHH1:CHH2 was 1:4 in both females and males, rendering CHH2 the major isoform.

3.2. MIH & CHH cDNA sequence analyses

The full-length *MIH* cDNA sequence (1561 bp, GenBank accession no. MK558261) includes a 454 bp 5′ UTR, a 342 bp ORF, and a 765 bp 3′ UTR (Fig. 2A). The ORF, encoding a MIH prohormone, consists of a 35-aa signal peptide (italicized) and a 78-aa mature hormone (underlined) (Fig. 2A). The deduced peptide sequence of MIH is depicted in a schematic diagram (Fig. 2B). The red crab MIH aa sequence is 86.7 % identical to *C. maenas* MIH (Q27225.1).

Phylogenetic analysis of MIH sequences placed *C. quinquedens* between two clades corresponding to Cancroidea and Portunoidae (Fig. 3). The Portunoidae MIHs formed a well-supported clade (0.97 bootstrap). The *C. quinquedens* MIH was sister to a weakly supported Cancroidae (0.72 bootstrap), which was grouped with weak bootstrap support (0.75) with Portunidae. Finally, these two clades were placed with strong support (0.99) with the last brachyuran clade, including *E. sinensis*, *Gecarcinus lateralis*, and *Discoplax celeste*. The outgroup consists of the clade containing lobster, shrimp, and crayfish.

The full-length cDNA sequence of *C. quinquedens* CHH (*CHH*: 957 bp, GenBank accession no. MG786421) contains a 5′ UTR (360 bp), an ORF (420 bp,) and a 3′ UTR (177 bp). The ORF finder predicts that the pre-prohormone encodes a 140-aa sequence containing a 20-aa signal peptide (italicized), 42-aa CPRP (dotted line), a dibasic cleavage site (KR)

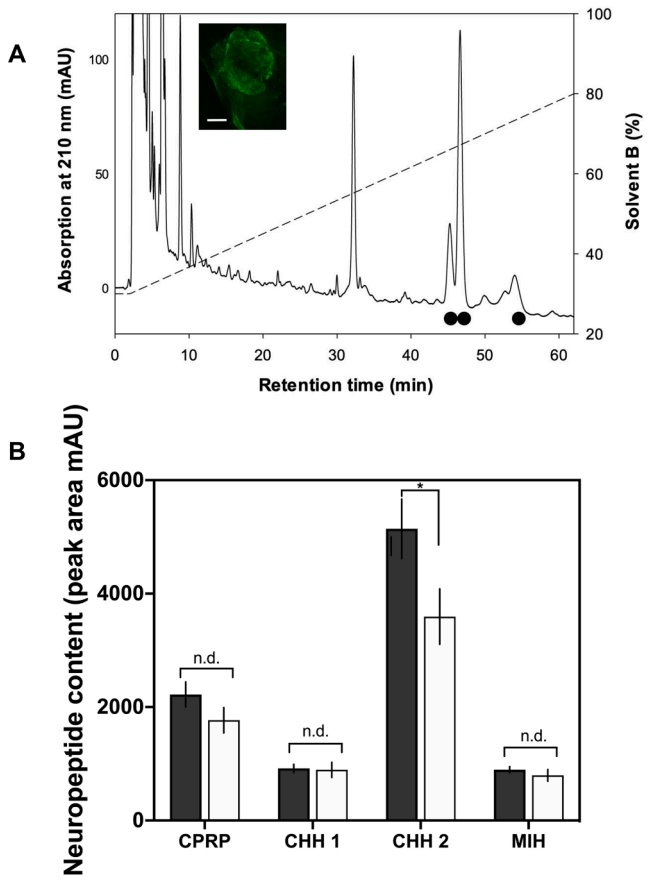

Fig. 1. Relative quantification of neuropeptide levels in the sinus gland of adult females and males. (**A**) A single sinus gland was separated on a C18 Gemini column with a gradient of 40–80 % B (0.1 % TFA in 60 % acetonitirle + 40 % water) over 60 min at 0.6 mL/min flow rate. The detection was at 210 nm wavelength that monitors peptide bonds. Neuropeptide peaks were identified as CHH 1, CHH 2, and MIH after identifying them with dot blot assays with specific antisera (noted with black dots). The inset shows a SG with CHH immunostaining (scale bar = 100 μm). (**B**) Neuropeptide content (peak area) for CPRP, CHH1, CHH2, and MIH of the females (closed bars) and males (open bars). The data are presented as mean ± 1SE (n). A student's *t*-test was used to determine statistical significance at $P < 0.05$. Differences were indicated with "*".

(boxed), a 72-aa mature hormone (double underline), an amidation site (G) (circled), and a tribasic cleavage site (RKK) (boxed) followed by a stop codon (Fig. 4A). A schematic diagram shows the major components, including the signal peptide, CPRP, followed by the mature CHH peptide (Fig. 4B). The 5′ UTR contains several translation regulatory sites: two Terminal Oligopyrimidine Tracts (TOP), one upstream open reading frame (uORF), and one Gamma interferon activated inhibitor of Ceruloplasmin mRNA translation (GAIT element). No regulatory motifs were found in the 3′ UTR of the *CHH* sequence (Table 3). Its amino acid sequence is 90.14 % identical to *C. maenas* CHH (CAA35605.1).

Phylogenetic analysis of *C. quinquedens* CHH is more complex with multiple structural isoforms found in *Cancer productus* with four isoforms, *Pachygraspus marmoratus* with two, and within the genus *Homarus* with two (Fig. 5). The *C. quinquedens* CHH was placed outside a strongly supported clade (0.97) containing most portunids. The Portunidae was not strongly supported but was sister to a strongly supported Cancridae clade (0.91) and formed a monophyletic group with other brachyurans (0.98 support). However, aside from the Thoracotremata (0.76), the Cancridae, and most of the portunids, there was little resolution of the major brachyuran clades.

3.3. Transcript levels of MIH, CHH, and VTG using qPCR assays

The *MIH* transcripts of adult female eyestalks at ovarian stages 2–5 (n = 5/stage) were estimated using qPCR and compared with males (n = 7) (Fig. 6A). *MIH* transcripts increased from $4.3 \pm 1.1 \times 10^6$ transcripts/μg total RNA at stage 2 to $7.6 \pm 1.2 \times 10^6$ transcripts/μg total RNA at stage 3, although these did not differ statistically. However, stage 3 levels were significantly higher than stage 4 ($2.3 \pm 0.3 \times 10^6$ transcripts/μg total RNA) and stage 5 ($3.3 \pm 0.6 \times 10^6$ transcripts/μg total RNA). Adult male *MIH* expression averaged $4.0 \pm 1.2 \times 10^{6.}$ transcripts/μg total RNA and was high compared to females at stages 3–5.

CHH expression in the eyestalk ganglia of adult females at ovarian stages 2–5 (n = 5/stage) was also estimated (Fig. 6B). The CHH expression did not significantly differ among ovarian stages, varying from stage 2 with $4.6 \pm 0.9 \times 10^6$ transcripts/μg total RNA; $2.1 \pm 0.6 \times 10^6$ transcripts/μg total RNA at stage 3; $2.5 \pm 0.8 \times 10^6$ transcripts/μg total RNA at stage 4; and $3.3 \pm 0.1 \times 10^6$ transcripts/μg total RNA at stage 5. AK levels, as a reference gene, did not differ by stage, ranging from $2.5 \pm 0.6 \times 10^5$ transcripts/μg total RNA, the lowest at stage 2 to $5.5 \pm 0.6 \times 10^5$ transcripts/μg total RNA, the highest at stage 5.

The *VTG* transcripts in the hepatopancreas obtained from the same animals at ovarian stages 2–5 were measured (Fig. 6C). There was an increasing trend in *VTG* levels among ovarian stages 2, 3, and 4, although they did not differ significantly. At stage 2, VTG was $1.7 \pm 1.4 \times 10^7$ transcripts/μg total RNA at stage 3 with $5.6 \pm 0.2 \times 10^7$ transcripts/μg total RNA and stage 4 with $7.8 \pm 0.2 \times 10^7$ transcripts/μg total RNA. At stage 5, *VTG* decreased to $1.7 \pm 0.4 \times 10^7$ transcripts/μg total RNA, similar to ovarian stage 2. AK levels, as a reference gene, remained consistent through all stages, ranging from $1.1 \pm 0.4 \times 10^7$ transcripts/μg total RNA to $1.6 \pm 0.3 \times 10^7$ transcripts/μg total RNA.

3.4. Transcriptome: Quality of RNAseq, de novo assembly and differential expression analysis

The *de novo* assembly of the 37 million paired-end reads at stage 1 and 38 million pairs at stage 3 of eyestalk ganglia produced 159,079 contigs (isoforms) with 98,355 genes (Table 2). The assembly was aligned to the 1066 genes in the arthropod BUSCO reference, showing 77.1 % complete contigs of which 26.0 % were duplicated (Table 2) (C:77.1 %[S:51.1 %,D:26.0 %],F:13.4 %,M:9.5 %,n:1066). Alignment of reads back to the assembled transcriptome showed 84.8 % of stage 1 and 84.4 % of stage 3 reads were concordantly mapped. The number of differentially expressed genes with TPM values greater than one was 8,756 unique to stage 1 and 9,528 to stage 3, while 56,613 were shared (Supplemental data 3).

The *de novo* assembly contained 3 MIH isoforms, two of which contained full-length coding sequences (Supplemental data 4) and 7 CHH isoforms which differed only in their 3′ UTR length and sequence (Supplemental data 5). The MIH sequences found in the *de novo* assembly and the cloned MIH were identical in the ORF. Similarly, the cloned and assembled CHH ORF were identical.

3.5. Neuropeptide prediction

Twenty-eight neuropeptides out of 53 search candidates were identified from the *C. quinquedens* eyestalk Trinity assembly transcriptome based on high identity sequences and full-length matches with e-values<1e-30 (Supplemental data 6). These 28 varied expression levels with the highest TPM values of 1981.7 for neuroparsin to the lowest, 0.2 for bursicon α subunit (Table 4).

The TPM values of these 28 were compared at stages 1 and 3. The majority (17/28), including MIH, ranged from 0.75 to 1.3-fold change, considered constant (Table 4). Ten neuropeptides had TPM values higher at stage 3 than 1, ranging from the highest with a twofold change of bursicon α, CHH, adipokinetic hormone (AKH)/corazonin-like, RYamide, crustacean cardioactive peptide (CCAP), allatostatin C, to the least

A

>***Chaceon quinquedens MIH*** **(GenBank accession no. MK558261)**

```
1          tgggtggtgcgtggtgccctcggactcaagtagcggctaactcaagggagtaccttgaggt
62         ggaccttgggagggtacacgtggtcaccgcctcgggtacacaagggcgcttcgataacgg
122        caagggcttggagtacacacaggcttatatgctggaatactggcgtcccggcctggcctc
182        cttcagggtctacatcagcggtcacggcaaccagacgttccaaggtaacatcaacaccta
242        cctggagcagaggaatgtgttggtacccccctctagtggccagcaaggtgcgcttcatacc
302        tgtctcctcccactcactcctcagcgtccctcatcctcccgccccgccactcacctcacg
362        ccgctcctgccctttcctcagtcctcctgtggctcccctccgttcacgcctccgtcaccc
422        agagctcgcctgtgagaggtcgtcagaagcatcATGatgtcccgcgctaactccagattt
                                          M  M  S  R  A  N  S  R  F  9
482        tcctgtcagaggacgtggctgctatctgtggtggtgctggccgcactttggagcttcagt
            S  C  Q  R  T  W  L  L  S  V  V  V  L  A  A  L  W  S  F  S  29
542        gtccagcgagcagcggcgagagttatcagcgacgactgtccaaaccttatcgggaacaga
            V  Q  R  A  A  A  R  V  I  S  D  D  C  P  N  L  I  G  N  R  49
602        gacctttataagaaagtagagtggatctgcgaagactgttcaaacatcttccgcaacaca
            D  L  Y  K  K  V  E  W  I  C  E  D  C  S  N  I  F  R  N  T  69
662        ggaatgactagtctttgcagaaagaactgcttctttaacgaggacttcctgtggtgtgtg
            G  M  T  S  L  C  R  K  N  C  F  F  N  E  D  F  L  W  C  V  89
722        tacgctacggagcggtccgaagagatgacacagttgaagcggtgggtcagcatcctggga
            Y  A  T  E  R  S  E  E  M  T  Q  L  K  R  W  V  S  I  L  G  109
782        gccggccgggacTGAgcggtgtcatctctccctccctcctcatggacgctgccgctgaat
            A  G  R  D  *                                               113
842        ctcacaccgatactgccaatcctacaagcactttataatgttgaaagtgaagtacctccc
902        tctctccctcagtgacgggctttgaacgactgaatcaagtgtaggaactcagcggcacct
962        acccttgtttcttatgatgagttcggtgtttgtggaactgttaacttatttattacgtg
1022       ccatttatgtaggtatttatttttactccataattcatttcgttctatgttaatttatcgc
1082       catctttgtcttaagtcttcatatttatgttacaaagaagttgatgaggtatttttagat
1142       gtgtgtgagtgtgtgtgtgttgtaataattggtctctgtaactgctgatgtgtccccgta
1202       gctggtgaccggaagcttgtatcgagaagagacagtaggggaagaaggaggagaaggagg
1262       aaaaggagaaggaaaagagaaataagagaagtagaggaagataaggaaagatatgtaagc
1322       taaaagacatttaattcaaccagtattctcaaactctagtcacgagtgatgatgcttcta
1382       gcgtctttgatattaatttgtgtcatattgatatttcgtgtttgtgttttgtagcatgta
1402       atgtgtgattttacgtttttttctatttagttataactgagctgctgcgttcttccacgca
1462       ttgtatttattatgatactgataaataaataaagtgcccgagaaaaaaaaaaaaaaaaaa
```

B

Fig. 2. Nucleotide and amino acid sequence of ChqMIH. (**A**) The full-length MIH cDNA sequence of *C. quinquedens* (*ChqMIH*, MK558261). The numbers on the left-hand side correspond to nucleotides and those on the right-hand side to the putative amino acid sequence of CHH identified using ORF finder (http://www.ncbi.nlm.nih.gov/projects/gorf/). The start codon (ATG) is shown in bold and capitalized. The 35 aa signal peptide was predicted by Signal P (http://www.cbs.dtu.dk/services/SignalP/) is italicized. The putative MIH is noted in bold and has a bold underline, and the stop codon is bolded and capitalized (TGA) marked with "*" underneath. **(B)** A schematic diagram of the putative MIH with numbers for the position of aa: the signal peptide: 1–35; and mature MIH: 36–113.

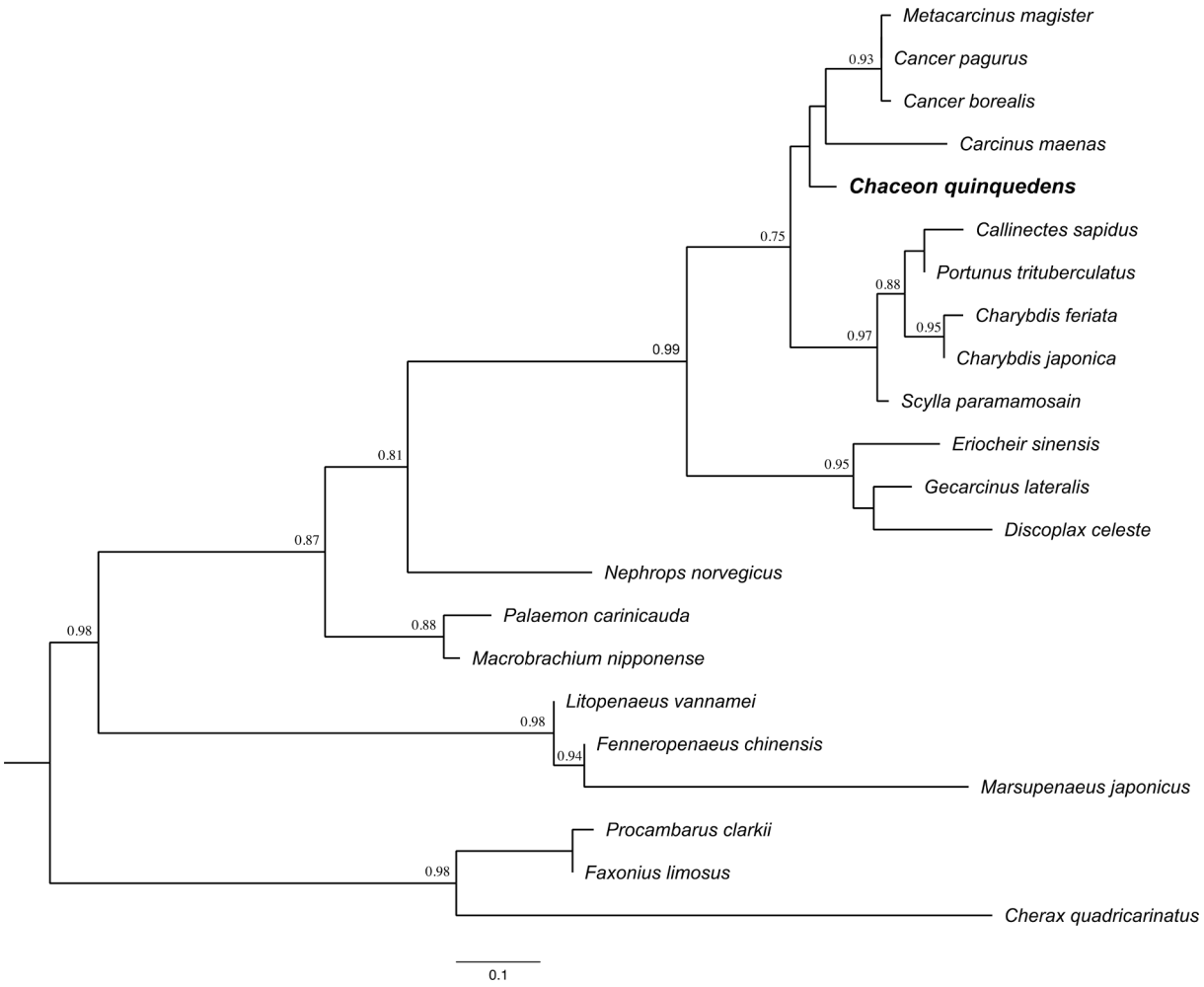

Fig. 3. Phylogenetic tree of MIH amino acid sequence of *C. quinquedens* and other decapods. A multiple sequence alignment of MIH amino acid sequences from other decapods and *C. quinquedens* (Supplemental data 1A) was used to generate a phylogenetic tree using Phylogeny fr. ChqMIH sequence is bolded. In brief, sequences were aligned using MUSCLE, trimmed with GBLOCKS, and the tree was built with PhyML.

with 1.37, IDLSRF-like peptide, allatostatin A, and PDH1. WXXXRamide was downregulated by ~ 2-fold at stage 3 compared to stage1 (Table 4).

4. Discussion

Large red deep-sea crab, *C. quinquedens* of the Geryonidae family, spends up to 7 years at the intermolt stage, with a long molt cycle (Gerrior, 1981; Lux et al., 1982), suggesting that this species is a k-selection strategist (Taylor and Roterman, 2017). A biannual reproductive cycle was proposed for adult females (Martínez-Rivera et al., 2020; Stevens and Guida, 2016). Interestingly, no adult females at the pre-vitellogenic stage are found in this study as stage 1 is noted as early vitellogenic (Haefner, 1978). These animals with an intermolt stage lasting up to 7 years could undergo at least three separate, continuous vitellogenesis events within a single molt cycle. Interestingly, *C. sapidus* adult females experiencing puberty-terminal molting stay at the permanent intermolt stage. In such cases, MIH exerts a dual function in holding the animals at the intermolt stage while actively stimulating vitellogenesis (Zmora et al., 2009b, Zmora et al., 2009a).

In decapod crustaceans, the molt cycle is regulated mainly by two neuropeptide hormones produced in eyestalk ganglia: MIH and CHH (Webster et al., 2012; Chen et al., 2020; Mykles and Chang, 2020). Hence, these two neuropeptides were considered for their potential role in the reproduction of *C. quinquedens* adult females. First, their levels were measured in the eyestalk with HPLC and immunostaining of the sinus gland. Then the cDNA for these two neuropeptide hormones were cloned, sequenced, and transcript levels measured with qPCR across four different ovarian stages. Finally, transcriptomics of female *C. quinquedens* eyestalk ganglia, the neuropeptide hub, at two ovarian stages was also used to provide a broad view of neuropeptides in *C. quinquedens*. The overall goal is to compare these results with the established roles of CHH and MIH in other valuable crustacean species.

Hundreds of CHH family neuropeptides are deposited in GenBank, with significantly higher numbers of CHH than MIH, most of which are reported from warm-water crustacean species. The phylogenetic position with *C. borealis*, *C. maenas*, and *Metacarcinus magister*, *Chaceon* MIH is closely related to an intertidal species, *C. maenas*, with an 87 % sequence identity. *C. quinquedens* CHH sequence is grouped with other cold-water crabs (Fig. 5), such as snow and cancer crab species. Like MIH, *C. quinquedens* CHH is most closely related to *C. maenas* with a 90 % sequence identity.

Like some crab species, *C. sapidus, C. maenas*, and *C. bairdi*, *Chaceon* SG has two forms of CHH (1 and 2) at a 1:4 ratio, with CHH2 as the major form (Chung et al., 2009; Jia et al., 2012). Interestingly, this ratio of 1:4 of CHH1:CHH2 is higher than other species, including *C. sapidus* at 1:5; *C. maenas* at 1:8; and *C. pagurus* at 1:10 (Chung et al., 1998; Chung and Webster, 2003), possibly due to a slower conversion of glutamine to pyroglutamate at the *N*-terminus of CHH primary sequence. Notably, CHH2 content in the SG of *C. quinquedens* differs by gender of the animals with the same size as it was consistently higher in *C. quinquedens*

A

>*Chaceon quinquedens CHH* (GenBank accession no. MG786421)

```
1     gtatatatattataaaatttacacacaaaaaagatatatgcatgagtatgccccgatata
61    taggtgacactatagagaatacacgatatatatataccgcgcggggagatctctcatata
121   ttggagacgcacgcgggcgcgagtacactagagagtgagcacagggatatatacagagag
181   tgcgggcgcgcacacacacacacacacacacacacacacacacacacacacacacacaca
241   cacacactaacacacacacgcacatatcctcttcttgaataccttaatgtttgaccatct
301   ctctctctctctctctctctctctctctctctctctctctctctctcagaacagcttccccc
361   ATGatggcagtactggtaatggtgtgcgtattcatgtacacactaccaaacgcacacgcc
          M  M  A  V  L  V  M  V  C  V  F  M  Y  T  L  P  N  A  H  A  20
421   cgatcagcgcaaggattaagaatggagcggcttttggcttcactgcgaggcccatcggac
          R  S  A  Q  G  L  R  M  E  R  L  L  A  S  L  R  G  P  S  D  40
481   accgcatctccccttggggatttcagcggctctagtaatcagggctcatcctctcacccc
          T  A  S  P  L  G  D  F  S  G  S  S  N  Q  G  S  S  S  H  P  60
541   ttggagaagcgacagatttacgacacgtcctgcaagggagtgtatgaccgtggcctgttc
          L  E  K  R  Q  I  Y  D  T  S  C  K  G  V  Y  D  R  G  L  F  80
601   agcgacctggagcatgtgtgtgacgactgctacaacctctaccgtacctcctacgtggcc
          S  D  L  E  H  V  C  D  D  C  Y  N  L  Y  R  T  S  Y  V  A  100
661   agtgcttgcagatcggactgctacagtaacttggtgttccggcaatgtatgaacgacctc
          S  A  C  R  S  D  C  Y  S  N  L  V  F  R  Q  C  M  N  D  L  120
721   ctcctcatggaagactttgaccagtacgccggaagagtacagatggttggaaggaagaag
          L  L  M  E  D  F  D  Q  Y  A  G  R  V  Q  M  V  G  R  K  K  140
781   TAGaatgtctatataatattgctacagtactagagctctccccctatcgcctctcacaac
          *
841   acgggaaagagagttataaatgcctatataatattactattccctccccatatcgcctct
901   cacaagtgccaaatattagagaaagagcaaaaaaaaaaaaaaaaaaaaaaaaaaaaaa
```

B

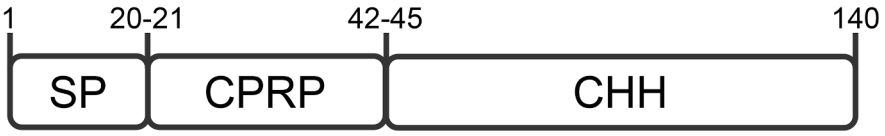

Fig. 4. Nucleotide and amino acid sequence of ChqCHH. (**A**) The full-length CHH cDNA sequence of *C. quinquedens* (*ChqCHH*, MG786421). The numbers on the left-hand side correspond to nucleotides and those on the right-hand side to the putative amino acid sequence of CHH identified using ORF finder (http://www.ncbi.nlm.nih.gov/projects/gorf/). The start codon (ATG) is bolded and capitalized. The 20 aa signal peptide was predicted by Signal P (http://www.cbs.dtu.dk/services/SignalP/) is italicized. The putative CPRP (42 aa) has a dotted underline. A dibasic cleavage site (KR) is boxed. The putative CHH is noted in bold and has a double underline, together with amidation site (G) which is also circled, a boxed tribasic cleavage site (RKK) and the stop codon is bolded (TAG) marked with "*". (**B**) A schematic diagram of the putative prepro CHH numbers for the position of aa: the signal peptide: 1–20; CPRP: 21–42; a dibasic cleavage site: 43–44; and CHH: 45–140.

females than in males. This contrasts with *C. maenas,* where the SG of the same-sized males and females contains similar CHH amounts (Chung and Webster, 1996).

Hormones involved in energy metabolism tend to accumulate in the glands of crustaceans and insects. For example, in decapod crustaceans, the CHH tends to accumulate in the SG throughout the life cycle of *C. sapidus* (Chung, unpublished data) starting with first detection in early embryogenesis (Chung and Webster, 2004; Techa et al., 2015). Interestingly, the adipokinetic hormone involved in insect lipid mobilization shows a similar accumulation pattern in the *corpora cardiaca* of

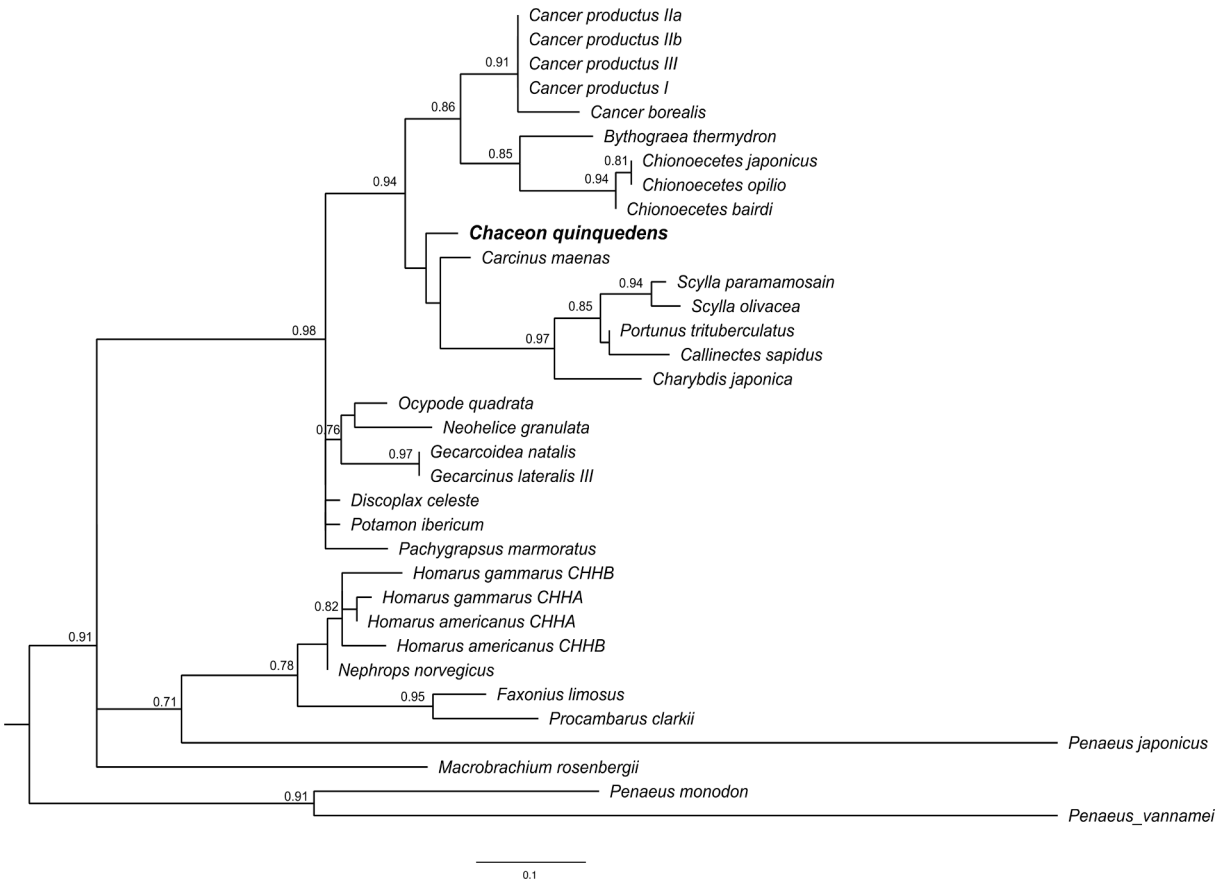

Fig. 5. Phylogenetic tree of eyestalk CHH amino acid sequence of *C. quinquedens* and of other decapods. A multiple sequence alignment of eyestalk CHH amino acid sequences from other decapods and *C. quinquedens* (Supplemental data 1B) was used to generate a phylogenetic tree using Phylogeny fr. ChqCHH sequence is bolded. In brief, sequences were aligned using MUSCLE, trimmed with GBLOCKS, and the tree was built with PhyML.

Locusta migratoria (O'Shea and Rayne, 1992). Insect corpora cardiaca, a tissue equivalent to the SG in decapod crustaceans. Therefore, it seems that Arthropod metabolic hormones like CHH and AKH are synthesized more than required, with a tendency to accumulate in the storage and release site of the SG and corpora cardiaca in crustaceans and insects, respectively.

The analysis of the 5′ and 3′UTR suggests that *Chaceon* CHH contains several potential regulatory sites in 5′UTR but none in the 3′UTR. This finding agrees with earlier reports on other cold-water crab species, *Chionoecetes* spp. (Chung et al., 2015, 2009). This further supports a potential translational regulation of CHH in the cold-water crustacean species (Chung et al., 2015), making the transcript levels less directly linked to protein levels. In contrast, MIH has no translation regulatory sites in the 5′ and 3′ UTRs in *C. quinquedens*, indicating that the transcription levels could reflect translation.

CHH transcripts measured with qPCR assay do not differ by ovarian stages. However, in transcriptome analysis, CHH has higher TPM values at stage 3 than 1 among neuropeptides with TPM values > 1. In this study, ovarian stage 1 samples had been used only for transcriptomic analysis, not for qPCR assays due to limited amounts of RNAs. CHH transcripts are the lowest at stage 3, compared to other stages (Fig. 6B). Therefore, it is reasonable to suggest that CHH transcripts at ovarian stages 2–5 could be significantly higher than at stage 1.

The potential translation regulatory sites in the 5′UTR of CHH cDNA sequence suggest that there may be translational regulation of *Chaceon* CHH mRNAs. Hence, transcription levels may not intimately reflect the neuropeptide levels. Moreover, the neuropeptide levels present in the SG do not equate with the translation levels in the neurosecretory cells. This is because the SG is the site for storing and releasing the eyestalk neuropeptides, as stated earlier. However, the difference in CHH neuropeptide levels in the SG at different ovarian stages indicates the levels of its release into the hemolymph, given that the transcript levels do not differ significantly. On the other hand, significant changes in MIH transcript levels in eyestalk ganglia but not neuropeptide levels in the SG were found at different ovarian stages.

The hepatopancreas, the primary tissue for vitellogenesis, contributes $>$ 99 % of VTG for ovarian development in crabs, including *C. quinquedens* and *C. sapidus* (Huang et al., 2020; Zmora et al., 2007). MIH and CHH hemolymph levels are not measured in this study. However, their levels, specifically MIH, would be high as all the females were at the intermolt stage, as reported (Zmora et al., 2009a). Additionally, it is proposed that in *C. quinquedens* with such an extended intermolt stage, MIH and CHH, usually found in high concentrations at the intermolt stage to halt the molt cycle, may act as a VSH/GSH in VTG synthesis of the hepatopancreas.

The *C. quinquedens* eyestalk transcriptome provided a more comprehensive picture of the various hormones and their expression at different vitellogenic stages. A particular interest is investigating genes expressed in stage 1 females which are harder to access due to fishery regulation and depth limits. The *C. quinquedens de novo* assembly is validated with high BUSCO scores (77.1 %) compared to the arthropod genes.

The *C. quinquedens* eyestalk assembly does not contain a GIH/VIH or GSH/VSH neuropeptide. The absence of GIH/VIH form in the assembly is confirmed in the simple SG chromatogram shown in Fig. 1A. Moreover, *C. quinquedens* CHH and or MIH may be multifunctional and act as a GIH/VIH or GSH/VSH. On the other hand, the assembly has several potentially reproductive hormones, as in the transcriptome of lobsters, shrimp, crabs, crayfish, and crayfish (Lv et al., 2017; Nguyen et al., 2016; Pang et al., 2019; Wei et al., 2020). Similar to studies that were

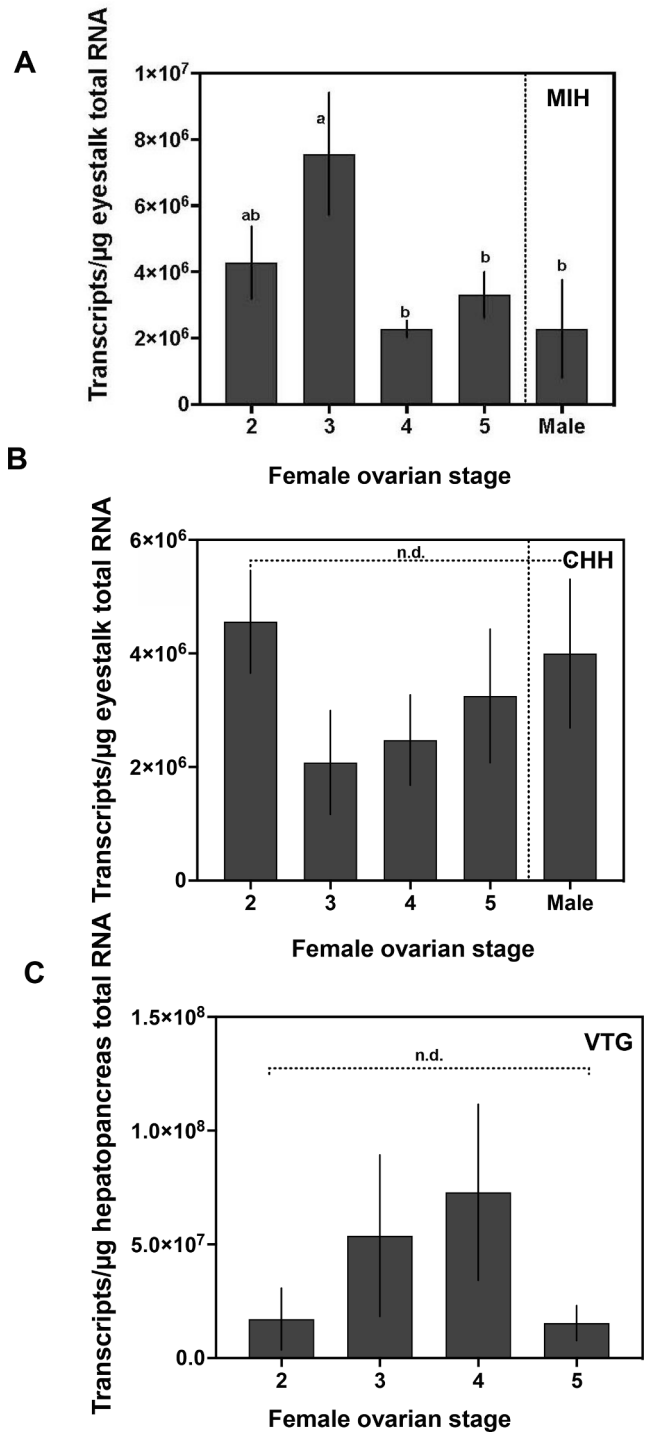

Fig. 6. Neuropeptide and vitellogenin expression levels from *C. quinquedens* adult females. Expression levels of eyestalk MIH (**A**) and CHH (**B**) in adult females (ovarian stages 2–5) and adult males. (**C**) Expression levels of vitellogenin in female (ovarian stages 2–5) hepatopancreas. All data are shown as mean ± 1 SE transcripts/µg total RNA (n = 5). Each cDNA sample was assayed in duplicate. Statistical significance was established using a non-parametric one-way analysis of variance (ANOVA) (Kruskal-Wallis test). Statistical differences at $P < 0.05$ were indicated with different letters.

previously mined for potential neuropeptides (Christie, 2016, 2014a, 2014b, 2014c; Christie et al., 2008), our search yielded 28 eyestalk-borne neuropeptides. The inventory of *C. quinquedens* neuropeptides is similar to the one reported in the mud crab, *S. paramamosain* (Bao et al., 2015), with a particular finding of the neuropeptides WXXXRamide and

Table 2
Eyestalk transcriptome statistics.

Total reads Eyestalk Stage 1	74,613,704 (37,306,852 paired)
Total reads Eyestalk Stage 3	75,395,282 (37,697,641 paired)
Total	150,008,986
Percent GC	43.65
Isoform Statistics	
Number of transcripts	159,079
Average transcript size (bp)	652
N50	931
Total assembled bases	103,875,774
BUSCO	(C:77.1 %[S:51.1 %,D:26.0 %],F:13.4 %,M:9.5 %, n:1066)
Gene Statistics	
Total number of genes	98,335
Average gene size (bp)	598
N50	803
Total assembled bases	58,839,147

GSEFamide. Even hormones with similar TPM values at different ovarian stages could still have a role in vitellogenesis. This study focuses on the changes in TPMs by ovarian stages. CHH, the only neuropeptide, has higher TPM values at stage 3 than 1 among neuropeptides with TPM values > 100. Neuroparsin ranks at the top with the highest TPM values, remaining at the same levels at ovarian stages 1 and 3. The constant expression of neuroparsin in *C. quinquedens* suggests a role in vitellogenesis and warrants further study to determine if it plays a negative role as seen in other decapods (Badisco et al., 2011; Liu et al., 2020; Yang et al., 2014).

CFSH is the fourth most highly expressed reproductive neuropeptide in the *Chaceon* transcriptome. In *C. quinquedens*, CFSH is slightly higher in eyestalks of females at ovarian stage 1. The function of CFSH, first reported in *C. sapidus*, is required for developing adult-specific morphological features for mating and brooding embryos (Zmora and Chung, 2014). *Chaceon,* belonging to pleocyemata, also broods embryos for their development up to 9–10 months until hatching (Elner et al., 1987; Haefner, 1978); it is reasonable to suggest that CFSH has the same functions as found in other crab species (Jiang et al., 2020; Zmora and Chung, 2014).

In *C. quinquedens*, MOIH is not found in the SG or *de novo* assembly. This is not unusual as MOIH is found only in Cancridae crabs (Chung et al., 2020; Wainwright et al., 1996). However, *de novo* assembly contains several insect allatostatins that is equivalent to crustacean MOIH, inhibiting methyl farnesoate (MF) synthesis by the mandibular organ (Wainwright et al., 1996). Therefore, further studies are needed to test if allatostains function as a MOIH in decapod crustaceans that do not possess MOIH.

5. Conclusion

The current study reports the isolation of *MIH* and *CHH* cDNA sequences, their expression levels, and the presence of MIH and CHH neuropeptide in the eyestalk ganglia-SG complex. The transcriptome of female eyestalk ganglia also contains other neuropeptides that show different TPM values by ovarian stages. Both MIH and CHH, traditionally known to display molt-inhibiting activity, may play an important role in the vitellogenesis of females in species such as *C. quinquedens* with long intermolt periods (2–7 years). In future studies, hemolymph titers of MIH and CHH need to be determined throughout ovarian development to define further their role in vitellogenesis and reproduction in this species.

CRediT authorship contribution statement

Shadaesha Green: Visualization, Writing – original draft, Writing –

Table 3
Comparison of putative translational regulatory sites in the 5′ and 3′ UTR of cold and warm water decapods (RegRNA analysis).

	Regulatory sites in 5′UTR				Regulatory sites in 3′UTR		
Species	**TOP**	**IRES**	**uORF**	**GAIT**	**GAIT**	**SECIS-T1**	**CPE**
C. quinquedens	**2**		**1**	**1**			
C. bairdi	**2**						
C. japonicus	**5**		**1**	**1**	**1**		
C. opilio	**5**		**1**	**1**	**1**		
C. sapidus							
S. paramamosain	**1**				**3**	**1**	**1**
S. olivacea		**1**		**1**	**8**	**1**	**1**

TOP = Terminal Oligopyrimidine Tract; IRES = Internal Ribosome Entry Site; GAIT = Gamma interferon activated inhibitor of Ceruloplasmin mRNA translation; SECIS-T1 = Selenocysteine Insertion Sequence Type 1; and CPE = Cytoplasmic polyadenylation element.

Table 4
Eyestalk neuropeptides identified from eyestalk transcriptome of *C. quinquedens*.

Neuropeptide name	TPM (stage)		TPM fold change	bit score	Trinity ID
	1	3			
Neuroparsin	1981.7	2138.0	1.08	115	DN72010_c0_g1_i1
Corazonin	649.7	536.9	0.83	162	DN1204_c0_g1_i2
EH	499.6	470.7	0.94	195	DN45_c0_g1_i5
PDH1	**329.8**	**452.0**	**1.37**	576	DN21903_c0_g2_i1
CCAP	**260.1**	**397.7**	**1.53**	245	DN16410_c0_g1_i1
MIH	223.7	168.5	0.75	207	DN3681_c0_g1_i1
DH31	146.3	165.9	1.13	186	DN7150_c0_g1_i2
CHH	**107.4**	**193.7**	**1.80**	177	DN365_c0_g1_i6
Orcokinin	97.8	103.2	1.06	186	DN2600_c0_g3_i1
SIFamide	89.8	81.2	0.90	92.8	DN701_c7_g1_i1
Myosuppressin	75.7	76.4	1.01	133	DN1178_c0_g1_i1
IDLSRF-LP	**47.8**	**65.5**	**1.37**	**307**	DN4730_c0_g1_i3
Tachykinin	39.4	46.1	1.17	142	DN8282_c0_g1_i1
CFSH	38.0	31.8	0.83	446	DN51890_c0_g1
Short NPF	**26.2**	**34.6**	**1.32**	92.8	DN4036_c0_g1_i1
Allotostatin B	20.5	21.6	1.05	479	DN2210_c0_g1_i7
FLRFamide	14.5	17.8	1.23	562	DN8457_c0_g1_i2
Allatostatin C	13.2	11.5	0.88	180	DN7628_c0_g1_i3
Allatostatin A	**10.6**	**14.0**	**1.32**	222	DN1313_c1_g1_i4
Glycoprotein B	**11.0**	**15.4**	**1.40**	234	DN7316_c0_g1_i5
GSEFLamide	9.7	9.3	0.96	345	DN11505_c0_g1_i15
RYamide	8.0	6.2	0.78	164	DN7666_c0_g2_i1
AKH/ corazonin-like	**4.3**	**7.6**	**1.75**	148	DN3516_c1_g1_i1
Pyrokinin	**5.6**	**8.9**	**1.59**	120	DN3453_c0_g4_i1
Glycoprotein A2	3.7	2.8	0.74	214	DN6268_c2_g1_i1
NPF1	3.6	4.5	1.26	137	DN4769_c0_g1_i2
WXXXRamide	***3.5***	***1.9***	***0.55***	538	DN11635_c0_g1_i1
Bursicon alpha	**0.2**	**0.4**	**2.00**	100	DN60850_c0_g1_i1

Ten peptides in bold typeset show higher TPM values at stage 3 than 1.
Abbreviations: EH = eclosion hormone; DH = diuretic hormone; CCAP = crustacean cardioactive peptide; AKH = adipokinetic hormone; PDH1 = pigment-dispersing hormone 1; NPF = neuropeptide F.

review & editing. **Tsvetan Bachvaroff:** Data curation, Software, Writing – review & editing. **J. Sook Chung:** Conceptualization, Data curation, Project administration, Resources, Supervision, Validation, Writing – original draft, Writing – review & editing.

Declaration of Competing Interest

The authors declare that they have no known competing financial interests or personal relationships that could have appeared to influence the work reported in this paper.

Data availability

Sequencing data are deposited to GenBank and will be available upon publication.

Acknowledgements

We appreciate the help given by the captains and crew members on board the NOAA R/V Gordan Gunter and the Atlantic Red Crab Company F/V Hannah Boden for their assistance with obtaining crab samples for this study. This study was supported by the National Oceanic and Atmospheric Administration, Office of Education Educational Partnership Program award number (NA11SEC4810002). Its contents are solely the responsibility of the award recipient and do not necessarily represent the official views of the U.S. Department of Commerce, National Oceanic and Atmospheric Administration.

Data availability

The RNA sequencing data sets have been submitted to NCBI Sequence Read Archive (SRA) under the BioProject PRJNA765736.

Appendix A. Supplementary data

Supplementary data to this article can be found online at https://doi.org/10.1016/j.ygcen.2022.114128.

References

Badisco, L., Marchal, E., van Wielendaele, P., Verlinden, H., Vleugels, R., vanden Broeck, J., 2011. RNA interference of insulin-related peptide and neuroparsins affects vitellogenesis in the desert locust *Schistocerca gregaria*. Peptides 32. https://doi.org/10.1016/j.peptides.2010.11.008.

Bao, C., Yang, Y., Huang, H., Ye, H., 2015. Neuropeptides in the cerebral ganglia of the mud crab, *Scylla paramamosain*: transcriptomic analysis and expression profiles during vitellogenesis. Sci. Rep. 5 https://doi.org/10.1038/srep17055.

Chan, S.-M., Chu, K., Tobe, S., 2003. Crustacean hyperglycemic genes of the CHH/MIH/GIH family: implications from molecular studies. Gen. Comp. Endocrinol. 134, 214–219.

Chen, T., Ren, C., Jiang, X., Zhang, L., Li, H., Huang, W., Hu, C., 2018. Mechanisms for type-II vitellogenesis-inhibiting hormone suppression of vitellogenin transcription in shrimp hepatopancreas: Crosstalk of GC/cGMP pathway with different MAPK-dependent cascades. PLoS ONE 13. https://doi.org/10.1371/journal.pone.0194459.

Chen, H.Y., Toullec, J.Y., Lee, C.Y., 2020. The crustacean hyperglycemic hormone superfamily: Progress made in the past decade. Front. Endocrinol. 11, 578958.

Chen, T., Zhang, L.-P., Wong, N.-K., Zhong, M., Ren, C.-H., Hu, C.-Q., 2014. Pacific white shrimp (*Litopenaeus vannamei*) vitellogenesis-inhibiting hormone (VIH) Is predominantly expressed in the brain and negatively regulates hepatopancreatic vitellogenin (VTG) gene expression. Bio. Reprod. 90, 1–10. https://doi.org/10.1095/biolreprod.113.115030.

Christie, A.E., 2014a. Prediction of the peptidomes of *Tigriopus californicus* and *Lepeophtheirus salmonis* (Copepoda, Crustacea). Gen. Comp. Endocrinol. 201, 87–106. https://doi.org/10.1016/j.ygcen.2014.02.015.

Christie, A.E., 2014b. Expansion of the *Litopenaeus vannamei* and *Penaeus monodon* peptidomes using transcriptome shotgun assembly sequence data. Gen. Comp. Endocrinol. 206, 235–254. https://doi.org/10.1016/j.ygcen.2014.04.015.

Christie, A.E., 2014c. Identification of the first neuropeptides from the Amphipoda (Arthropoda, Crustacea). Gen. Comp. Endocrinol. 206, 96–110. https://doi.org/10.1016/j.ygcen.2014.07.010.

Christie, A.E., 2015. Neuropeptide discovery in *Symphylella vulgaris* (Myriapoda, Symphyla): In silico prediction of the first myriapod peptidome. Gen. Comp. Endocrinol. 223, 73–86. https://doi.org/10.1016/j.ygcen.2015.09.021.

Christie, A.E., 2016. Expansion of the neuropeptidome of the globally invasive marine crab *Carcinus maenas*. Gen. Comp. Endocrino. 235, 150–169. https://doi.org/10.1016/j.ygcen.2016.05.013.

Christie, A.E., Cashman, C.R., Stevens, J.S., Smith, C.M., Beale, K.M., Stemmler, E.A., Greenwood, S.J., Towle, D.W., Dickinson, P.S., 2008. Identification and cardiotropic actions of brain/gut-derived tachykinin-related peptides (TRPs) from the American lobster *Homarus americanus*. Peptides 29, 1909–1918. https://doi.org/10.1016/j.peptides.2008.07.010.

Christie, A.E., Pascual, M.G., 2016. Peptidergic signaling in the crab Cancer borealis: Tapping the power of transcriptomics for neuropeptidome expansion. Gen. Comp. Endocrinol. 237, 53–67. https://doi.org/10.1016/j.ygcen.2016.08.002.

Christie, A.E., Roncalli, V., Cieslak, M.C., Pascual, M.G., Yu, A., Lameyer, T.J., Stanhope, M.E., Dickinson, P.S., 2017. Prediction of a neuropeptidome for the eyestalk ganglia of the lobster *Homarus americanus* using a tissue-specific de novo assembled transcriptome. Gen. Comp. Endocrinol. 243, 96–119. https://doi.org/10.1016/j.ygcen.2016.11.001.

Chung, J.S., 2004. Expression and release patterns of neuropeptides during embryonic development and hatching of the green shore crab, *Carcinus maenas*. Development 131, 4751–4761. https://doi.org/10.1242/dev.01312.

Chung, J., Christie, A., Flynn, E., 2020. Molecular cloning of crustacean hyperglycemic hormone (CHH) family members (CHH, molt-inhibiting hormone and mandibular organ-inhibiting hormone) and their expression levels in the Jonah crab. *Cancer borealis*. Gen. Comp. Endocrinol. 295, 113522 https://doi.org/10.1016/j.ygcen.2020.113522.

Chung, J.S., Katayama, H., Dircksen, H., 2012. New functions of arthropod bursicon: inducing deposition and thickening of new cuticle and hemocyte granulation in the blue crab. *Callinectes sapidus*. PLoS ONE 7. https://doi.org/10.1371/journal.pone.0046299.

Chung, J.S., Webster, S.G., 1996. Does the N-terminal pyroglutamate residue have any physiological significance for crab hyperglycemic neuropeptides? Eur. J. Biochem. 240, 358–364. https://doi.org/10.1111/j.1432-1033.1996.0358h.x.

Chung, J.S., Ahn, I.S., Yu, O.H., Kim, D.S., 2015. Crustacean hyperglycemic hormones of two cold water crab species, *Chionoecetes opilio* and *C. japonicus*: isolation of cDNA sequences and localization of CHH neuropeptide in eyestalk ganglia. Gen. Comp. Endocrinol. 214, 177–185. https://doi.org/10.1016/j.ygcen.2014.08.017.

Chung, J.S., Webster, S.G., 2003. Moult cycle-related changes in biological activity of moult-inhibiting hormone (MIH) and crustacean hyperglycaemic hormone (CHH) in the crab, *Carcinus maenas*: from target to transcript. Eur. J. Biochem. 270, 3280–3288. https://doi.org/10.1046/j.1432-1033.2003.03720.x.

Chung, J.S., Webster, S.G., 2004. Expression and release patterns of neuropeptides during embryonic development and hatching of the green shore crab, *Carcinus maenas*. Development (Cambridge, England) 131, 4751–4761. https://doi.org/10.1242/dev.01312.

Chung, J.S., Wilkinson, C.M., Webster, S.G., 1998. Amino acid sequences of both isoforms of crustacean hyperglycemic hormone (CHH) and corresponding precursor-related peptide in *Cancer pagurus*. Reg. Pept. 77, 17–24. https://doi.org/10.1016/S0167-0115(98)00024-X.

Chung, J.S., Bembe, S., Tamone, S., Andrews, E., Thomas, H., 2009. Molecular cloning of the crustacean hyperglycemic hormone (CHH) precursor from the x-organ and the identification of the neuropeptide from sinus gland of the Alaskan Tanner crab, *Chionoecetes bairdi*. Gen. Comp. Endocrinol. 162, 129–133. https://doi.org/10.1016/j.ygcen.2009.03.012.

Chute, A., Jacobson, L., Rago, P., MacCall, A., 2008. Deep Sea red crab. Northeast Data Poor Stocks Working Group Meeting 1–18.

Elner, R.W., Koshio, S., Hurley, G.V., 1987. Mating behavior of the deep-sea red crab, *Geryon quinquedens* Smith (Decapoda, Brachyura, Geryonidae). Crustaceana 52, 194–201.

Erdman, R.B., Blake, N.J., Lockhart, F.D., Lindberg, W.J., Perry, H.M., Waller, R.S., 1991. Comparative reproduction of the deep-sea crabs *Chaceon fenneri* and *C. quinquedens* (Brachyura: Geryonidae) from the northeast Gulf of Mexico. Invert. Reprod. Dev. 19, 175–184.

Gao, J., Wang, X., Zou, Z., Jia, X., Wang, Y., Zhang, Z., 2014. Transcriptome analysis of the differences in gene expression between testis and ovary in green mud crab (*Scylla paramamosain*). BMC Genomics 15. https://doi.org/10.1186/1471-2164-15-585.

Gerrior, P., 1981. The distribution and effects of fishing on the deep-sea red crab, *Geryon quinquedens* Smith, off southern New England. North Dartmouth, MA.

Grabherr, M.G., Haas, B.J., Yassour, M., Levin, J.Z., Thompson, D.A., Amit, I., Adiconis, X., Fan, L., Raychowdhury, R., Zeng, Q., Chen, Z., Mauceli, E., Hacohen, N., Gnirke, A., Rhind, N., di Palma, F., Birren, B.W., Nusbaum, C., Lindblad-Toh, K., Friedman, N., Regev, A., 2011. Full-length transcriptome assembly from RNA-Seq data without a reference genome. Nature Biotechnol. 29, 644–652. https://doi.org/10.1038/nbt.1883.

Haas, B.J., Papanicolaou, A., Yassour, M., Grabherr, M., Blood, P.D., Bowden, J., Couger, M.B., Eccles, D., Li, B., Lieber, M., Macmanes, M.D., Ott, M., Orvis, J., Pochet, N., Strozzi, F., Weeks, N., Westerman, R., William, T., Dewey, C.N., Henschel, R., Leduc, R.D., Friedman, N., Regev, A., 2013. De novo transcript sequence reconstruction from RNA-seq using the Trinity platform for reference generation and analysis. Nature Protocols 8, 1494–1512. https://doi.org/10.1038/nprot.2013.084.

Haefner, P.A., 1977. Reproductive biology of the female Deep-Sea Red Crab, *Geryon quinquedens*, from the Chesapeake Bight. Fish. Bull. 75, 91–102.

Haefner, P., 1978. Seasonal aspects of the biology, distribution and relative abundance of the deep-sea red crab *Geryon quinquedens* Smith, in the vicinity of the Norfolk Canyon, Western North Atlantic. Proc. Nat. Shellfish. Assoc. 68, 49–62.

Haefner, P.A., Musick, J.A., 1974. Observations on distribution and abundance of red crabs in Norfolk Canyon and adjacent continental slope. Mar. Fish. Rev. 36, 31–34.

Hilário, A., Cunha, M.R., 2013. Notes on a mating event of the deep-sea crab *Chaceon affinis* in the Gorringe Bank (NE Atlantic). Deep-Sea Research Part II: Topical Studies in Oceanography 92, 58–62. https://doi.org/10.1016/j.dsr2.2013.01.021.

Huang, X., Green, S., Sook Chung, J., 2020. The presence of an insulin-like peptide-binding protein (ILPBP) in the ovary and its involvement in the ovarian development of the red deep-sea crab. *Chaceon quinquedens*. Gen. Com. Endocrinol. 301, 113653 https://doi.org/10.1016/j.ygcen.2020.113653.

Jia, C., Hui, L., Cao, W., Lietz, C.B., Jiang, X., Chen, R., Catherman, A.D., Thomas, P.M., Ge, Y., Kelleher, N.L., Li, N., 2012. High-definition de novo sequencing of Crustacean Hyperglycemic Hormone (CHH)-family neuropeptides. Mol. Cell. Proteomics 11, 1951–1964. https://doi.org/10.1074/mcp.M112.020537.

Jiang, Q., Lu, B., Lin, D., Huang, H., Chen, X., Ye, H., 2020. Role of crustacean female sex hormone (CFSH) in sex differentiation in early juvenile mud crabs. *Scylla paramamosain*. Gen. Com. Endocrinol. 289 https://doi.org/10.1016/j.ygcen.2019.113383.

Kluebsoongnoen, J., Panyim, S., Udomkit, A., 2020. Regulation of vitellogenin gene expression under the negative modulator, gonad-inhibiting hormone in *Penaeus monodon*. Comp. Biochem. Physiol. Part A: Mol. Integr. Physiol. 243, 110682.

Li, B., Dewey, C.N., 2011. RSEM: accurate transcript quantification from RNA-Seq data with or without a reference genome. BMC Bioinformatics. 12, 323.

Liu, J., Liu, A., Liu, F., Huang, H., Ye, H., 2020. Role of neuroparsin 1 in vitellogenesis in the mud crab. *Scylla paramamosain*. Gen. Com. Endocrinol. 285, 113248 https://doi.org/10.1016/j.ygcen.2019.113248.

Lux, F.E., Ganz, A.R., Rathjen, W.F., 1982. Marking studies on the red crab *Geryon quinquedens* Smith off southern New England. J. Shellfish Res. 2, 71–80.

Lv, J., Zhang, L., Liu, P., Li, J., 2017. Transcriptomic variation of eyestalk reveals the genes and biological processes associated with molting in *Portunus trituberculatus*. PLoS ONE 12. https://doi.org/10.1371/journal.pone.0175315.

Ma, M., Gard, A.L., Xiang, F., Wang, J., Davoodian, N., Lenz, P.H., Malecha, S.R., Christie, A.E., Li, L., 2010. Combining *in silico* transcriptome mining and biological mass spectrometry for neuropeptide discovery in the Pacific white shrimp Litopenaeus vannamei. Peptides 31, 27–43. https://doi.org/10.1016/j.peptides.2009.10.007.

Manfrin, C., Tom, M., de Moro, G., Gerdol, M., Giulianini, P.G., Pallavicini, A., 2015. The eyestalk transcriptome of red swamp crayfish *Procambarus clarkii*. Gene 557, 28–34. https://doi.org/10.1016/j.gene.2014.12.001.

Martínez-Rivera, S., Long, W.C., Stevens, B.G., 2020. Physiological and behavioral sexual maturity of female red deep-sea crabs *Chaceon quinquedens* (Smith, 1879) (Decapoda: Brachyura: Geryonidae) in the Mid-Atlantic Bight. J. Crust. Biol. 40, 330–340. https://doi.org/10.1093/jcbiol/ruaa007.

Martínez-Rivera, S., Stevens, B.G., 2020. Embryonic development and fecundity of the red deep-sea crab Chaceon quinquedens (Smith, 1879) (Decapoda: Brachyura: Geryonidae) in the Mid-Atlantic Bight determined by image analysis. J. Crust. Biol. 40, 230–236. https://doi.org/10.1093/jcbiol/ruaa017.

Meng, X.L., Liu, P., Jia, F.L., Li, J., Gao, B.Q., 2015. De novo transcriptome analysis of *Portunus trituberculatus* ovary and testis by RNA-Seq: Identification of genes involved in gonadal development. PLoS ONE 10. https://doi.org/10.1371/journal.pone.0128659.

Mykles, D.L., Chang, E.S., 2020. Hormonal control of the crustacean molting gland: Insights from transcriptomics and proteomics. Gen. Comp. Endocrinol. 294, 113493.

Nguyen, T.V., Cummins, S.F., Elizur, A., Ventura, T., 2016. Transcriptomic characterization and curation of candidate neuropeptides regulating reproduction in the eyestalk ganglia of the Australian crayfish, *Cherax quadricarinatus*. Sci. Rep. 6, 1–19. https://doi.org/10.1038/srep38658.

O'Shea, M., Rayne, R.C., 1992. Adipokinetic hormones: cell and molecular biology. Experientia 48, 430–438.

Y. Pang yang, Zhang, C., Xu, M. jie, Huang, G. yong, Cheng, Y. xu, Yang, X. zhen, The transcriptome sequencing and functional analysis of eyestalk ganglions in Chinese mitten crab (Eriocheir sinensis) treated with different photoperiods PLoS ONE 14 2019 1 18 10.1371/journal.pone.0210414.

Qiao, H., Fu, H., Xiong, Y., Jiang, S., Zhang, W., Sun, S., Jin, S., Gong, Y., Wang, Y., Shan, D., Li, F., Wu, Y., 2017. Molecular insights into reproduction regulation of female Oriental River prawns *Macrobrachium nipponense* through comparative transcriptomic analysis. Sci. Rep. 7, 1–11. https://doi.org/10.1038/s41598-017-10439-2.

Robinson, M.D., McCarthy, D.J., Smyth, G.K., 2010. edgeR: a Bioconductor package for differential expression analysis of digital gene expression data. Bioinformatics. 26, 139–140.

Rotllant, G., Nguyen, T.V., Hurwood, D., Sbragaglia, V., Ventura, T., Company, J.B., Joly, S., Elizur, A., Mather, P.B., 2018. Evaluation of genes involved in Norway lobster (*Nephrops norvegicus*) female sexual maturation using transcriptomic analysis. Hydrobiologia 825, 137–158. https://doi.org/10.1007/s10750-018-3521-3.

Serchuk, F.M., Wigley, R.L., 1982. Deep-sea red crab, *Geryon quinquedens*. Fish Distribution 15, 125–129.

Simão, F.A., Waterhouse, R.M., Ioannidis, P., Kriventseva, E.v., Zdobnov, E.M., 2015. BUSCO: Assessing genome assembly and annotation completeness with single-copy orthologs. Bioinformatics 31, 3210–3212. https://doi.org/10.1093/bioinformatics/btv351.

Stefanini, M., Demartino, C., Zamboni, L., 1967. Fixation of ejaculated spermatozoa for electron microscopy. Nature 216, 173–174.

F.W. Steimle C.A. Zetlin S. Chang Red deepsea crab, Chaceon (Geryon) quinquedens, life history and habitat characteristics NOAA Tech. Memo. 2001 NMFS-NE-163 1–27.

Stevens, B.G., Guida, V., 2016. Depth and temperature distribution, morphometrics, and sex ratios of red deepsea crab (*Chaceon quinquedens*) at 4 sampling sites in the Mid-Atlantic Bight. Fish. Bull. 114, 343–359. https://doi.org/10.7755/FB.114.3.7.

Suwansa-Ard, S., Thongbuakaew, T., Wang, T., Zhao, M., Elizur, A., Hanna, P.J., Sretarugsa, P., Cummins, S.F., Sobhon, P., 2015. In silico neuropeptidome of female *Macrobrachium rosenbergii* based on transcriptome and peptide mining of eyestalk,

central nervous system and ovary. PLoS ONE 10, 1–31. https://doi.org/10.1371/journal.pone.0123848.
Taylor, M.L., Roterman, C.N., 2017. Invertebrate population genetics across Earth's largest habitat: the deep-sea floor. Mol. Ecol. 26, 4872–4896. https://doi.org/10.1111/mec.14237.
Techa, S., Alvarez, J.v., Sook Chung, J., 2015. Changes in ecdysteroid levels and expression patterns of ecdysteroid-responsive factors and neuropeptide hormones during the embryogenesis of the blue crab, *Callinectes sapidus*. Gen. Comp. Endocrinol. 214, 157–166. https://doi.org/10.1016/j.ygcen.2014.07.017.
Tiu, S.-H.-K., Chan, S.-M., 2007. The use of recombinant protein and RNA interference approaches to study the reproductive functions of a gonad-stimulating hormone from the shrimp *Metapenaeus ensis*. The FEBS J. 274, 4385–4395.
Tsutsui, N., Nagakura-Nakamura, A., Nagai, C., Ohira, T., Wilder, M.N., Nagasawa, H., 2013. The ex vivo effects of eyestalk peptides on ovarian vitellogenin gene expression in the kuruma prawn *Marsupenaeus japonicus*. Fish. Sci. 79, 33–38. https://doi.org/10.1007/s12562-012-0566-5.
Ventura, T., Cummins, S.F., Fitzgibbon, Q., Battaglene, S., Elizur, A., 2014. Analysis of the central nervous system transcriptome of the Eastern rock lobster *Sagmariasus verreauxi* reveals its putative neuropeptidome. PLoS ONE 9. https://doi.org/10.1371/journal.pone.0097323.
Vijayan, K.K., Reynolds, P., Mohanlal, D.L., Balasubramanium, C.P., 2013. Preliminary characterisation of gonad inhibiting hormone (GIH) gene and its expression pattern during vitellogenesis in giant tiger shrimp, *Penaeus monodon* Fabricius, 1798. Indian J Fish. 60, 103–107.
Vinagre, A.S., Chung, J.S., 2016. Effects of starvation on energy metabolism and crustacean hyperglycemic hormone (CHH) of the Atlantic ghost crab *Ocypode quadrata* (Fabricius, 1787). Mar. Biol. 163 https://doi.org/10.1007/s00227-015-2797-3.
Vinagre, A.S., Model, J.F.A., Vogt, É.L., Manara, L.M., Trapp, M., da Silva, R.S.M., Chung, J.S., 2020. Diet composition and long-term starvation do not affect crustacean hyperglycemic hormone (CHH) transcription in the burrowing crab *Neohelice granulata* (Dana, 1851). Comp. Biochem. Physiol. Part A: Mol. Integrat. Physiol. 247. https://doi.org/10.1016/j.cbpa.2020.110738.
Wahle, R.A., Bergeron, C.E., Chute, A.S., Jacobson, L.D., Chen, Y., 2008. The Northwest Atlantic deep-sea red crab (*Chaceon quinquedens*) population before and after the onset of harvesting. ICES J. Mar. Sci. 65, 862–872.
Wainwright, G., Webster, S.G., Wilkinson, M.C., Chung, J.S., Rees, H.H., 1996. Structure and Significance of mandibular organ-inhibiting hormone in the crab, *Cancer pagurus*: involvement in multihormonal regulation of growth and reproduction. J. Biol. Chem. 271, 12749–12754.
Wang, Z., Luan, S., Meng, X., Cao, B., Luo, K., Kong, J., 2019. Comparative transcriptomic characterization of the eyestalk in Pacific white shrimp (*Litopenaeus vannamei*) during ovarian maturation. Gen. Comp. Endocrinol. 274, 60–72. https://doi.org/10.1016/j.ygcen.2019.01.002.
Webb, J.B., Eckert, G.L., Shirley, T.C., Tamone, S.L., 2007. Changes in embryonic development and hatching in *chionoecetes opilio* (snow crab) with variation in incubation temperature. Biol. Bull. 213, 67–75.
Webster, S.G., Keller, R., Dircksen, H., 2012. The CHH-superfamily of multifunctional peptide hormones controlling crustacean metabolism, osmoregulation, moulting, and reproduction. Gen. Comp. Endocrinol. 175, 217–233. https://doi.org/10.1016/j.ygcen.2011.11.035.
Wei, C., Pan, L., Zhang, X., Tong, R., 2020. Comparative transcriptome analysis of eyestalk from the white shrimp *Litopenaeus vannamei* after the injection of dopamine. Gene 763, 145115. https://doi.org/10.1016/j.gene.2020.145115.
Weinberg, J.R., Keith, C., 2003. Population size-structure of harvested deep-sea red crabs (*Chaceon quinquedens*) in the northwest Atlantic Ocean. Crustaceana 79, 819–833.
Wigley, R.L., Theroux, R.B., Murray, H.E., 1975. Deep-sea red crab, *Geryon quinquedens*, survey off northeastern United States. Mar. Fish. Rev. 1154, 1–22.
Xu, Z., Zhao, M., Li, K., Lu, Q., Li, Y., JGe, J, Pan, J., 2015. Transcriptome profiling of the eyestalk of precocious juvenile Chinese mitten crab reveals putative neuropeptides and differentially expressed genes. Gene. 569, 280–286.
Yang, S.P., He, J.-G., Sun, C.B., Chan, S.F., 2014. Characterization of the shrimp neuroparsin (MeNPLP): RNAi silencing resulted in inhibition of vitellogenesis. FEBS Open Bio 4. https://doi.org/10.1016/j.fob.2014.09.005.
Zhang, Y., Jiang, S., Qiao, H., Xiong, Y., Fu, H., Zhang, W., Gong, Y., Jin, S., Wu, Y., 2021. Transcriptome analysis of five ovarian stages reveals gonad maturation in female Macrobrachium nipponense. BMC Genomics 22. https://doi.org/10.1186/s12864-021-07737-5.
Zmora, N., Chung, J.S., 2014. A novel hormone is required for the development of reproductive phenotypes in adult female crabs. Endocrinology 155, 230–239. https://doi.org/10.1210/en.2013-1603.
Zmora, N., Trant, J., Chan, S.M., Chung, J.S., 2007. Vitellogenin and its messenger RNA during ovarian development in the female blue crab, *Callinectes sapidus*: Gene expression, synthesis, transport, and cleavage. Biol. Reprod. 77, 138–146. https://doi.org/10.1095/biolreprod.106.055483.
Zmora, N., Sagi, A., Zohar, Y., Chung, J.S., 2009a. Molt-inhibiting hormone stimulates vitellogenesis at advanced ovarian developmental stages in the female blue crab, *Callinectes sapidus* 2: novel specific binding sites in hepatopancreas and cAMP as a second messenger. Saline systems 5, 6. https://doi.org/10.1186/1746-1448-5-6.
Zmora, N., Trant, J., Zohar, Y., Chung, J.S., 2009b. Molt-inhibiting hormone stimulates vitellogenesis at advanced ovarian developmental stages in the female blue crab, *Callinectes sapidus* 1: an ovarian stage dependent involvement. Saline systems 5, 7. https://doi.org/10.1186/1746-1448-5-7.